Decitabine induces cell differentiation and growth inhibition accompanied by upregulation of microRNA-143 and MS4A3 in the myelodysplastic syndromes-derived leukemic cell line MDS-L

RIE NISHI[1], NAOKO HOSONO[1], KAORU THOYAMA[2] and TAKAHIRO YAMAUCHI[1]

[1]Department of Hematology and Oncology, Faculty of Medical Sciences, University of Fukui, Eiheiji, Fukui 910-1193, Japan; [2]Department of Laboratory Medicine, Kawasaki Medical School, Kurashiki, Okayama 701-0192, Japan

Received May 19, 2024; Accepted July 21, 2025

DOI: 10.3892/ol.2026.15873

Abstract. Myelodysplastic syndromes (MDS) are a group of clonal myeloid neoplasms characterized by ineffective hematopoiesis and cytopenia. Hypomethylating agents (HMAs) serve a central role in the treatment of high-risk MDS, but their mechanisms of action are diverse and not fully understood. To investigate the molecular mechanisms of HMAs, an MDS cell line (MDS-L) was cultured with a non-toxic concentration of decitabine (DAC) for 6 months and drug sensitivity, cell differentiation and DNA methylation profiles were evaluated. MDS-L cells with long-term exposure to DAC (MDS-L-DAC) were morphologically mature with nuclear lobulation and cytoplasmic granulation, accompanied by decreased expression levels of the CD34 surface antigen. MDS-L-DAC cells exhibited decreased Wilms tumor 1 (WT1) expression levels and increased induction of apoptosis by DAC. DNA methylation array analysis demonstrated the demethylation of membrane spanning 4-domains A3 (MS4A3) and microRNA-143 (miR143) in MDS-L-DAC cells. miR143 functions as a tumor suppressor through the MAPK/ERK pathway, and in MDS-L-DAC cells, decreased expression levels of KRAS and β-catenin were observed, associated with the increased expression of miR143. The differentiation of MDS cells and decreased expression levels of WT1 induced by long-term incubation with DAC may involve the restoration of function via demethylation of the miR143 and MS4A3 gene promoters, which could potentially contribute to eliminating the malignant phenotype through reductions in KRAS and β-catenin expression levels.

Correspondence to: Dr Naoko Hosono, Department of Hematology and Oncology, Faculty of Medical Sciences, University of Fukui, 23-3 Shimoaizuki, Matsuoka, Eiheiji, Fukui 910-1193, Japan
E-mail: hosono@u-fukui.ac.jp

Key words: decitabine, myelodysplastic syndromes, Wilms tumor 1, microRNA-143, membrane spanning 4-domains A3, β-catenin

Introduction

Myelodysplastic syndromes (MDS) are a heterogeneous group of clonal hematopoietic malignancies characterized by cytopenia, dysplasia, ineffective hematopoiesis and an increased risk of progression to acute myeloid leukemia (AML). The annual incidence of MDS in the USA is ~4/100,000 individuals, according to the United States Surveillance, Epidemiology, and End Results database (1). A large proportion of patients with MDS are elderly, with a median age at diagnosis of ~70 years (1) and are often not eligible for stem cell transplantation because of comorbidities, advanced age and/or the lack of a suitable transplant donor (2,3). The hypomethylating agents (HMAs) azacytidine and decitabine (5-aza-2'-deoxycytidine; DAC) are used to treat high-risk MDS and AML in patients who are not eligible for allogeneic hematopoietic cell transplantation (4,5).

HMAs can inhibit DNA methyltransferase (DNMT) activity and prevent the methylation of nascent strands after DNA replication; this epigenetic modification is reversible, as HMAs do not affect *de novo* DNMT synthesis (6,7). DAC is a pyrimidine nucleoside analog that enters the cell via the human equilibrative nucleoside transporters, human equilibrate nucleoside transporter 1 (hENT1) and hENT2. Once inside the cell, DAC is phosphorylated by the deoxycytidine kinase to generate DAC 5'-monophoshate, which is then converted to 5-aza-2'-deoxycytidine triphosphate (5-aza-dCTP), the active metabolite of DAC. Subsequently, 5-aza-dCTP competes with and replaces cytosine in cytosine-guanosine dinucleotide (CpG) islands, inhibiting promoter methylation and thus contributing to DNMT degradation (8-13). Therefore, DAC may induce DNA demethylation and restore the expression levels of multiple tumor suppressor genes [such as *BRCA1*, cadherin 1 and *FOXO* family genes (including *FOXO1* and *3A*)] that were silenced by abnormal methylation (14,15). Numerous studies identify methylation patterns that predict response to DAC (16,17). A retrospective analysis of the DNMT3A mutation status demonstrates a high response rate in a small cohort (the complete response rate was 75% in 6/8 cases), but this requires further validation in larger studies (18-20). The pretreatment levels of microRNA-29b (miR29b) have been reported to be associated with the response to DAC (21,22).

This is consistent as miR29b function to specifically inhibits DNMT1 expression; however, the association of miR29b levels with the response to HMAs could not be confirmed in another larger study (23). The exact mechanism of action of DAC is currently unknown, although several studies have been conducted to identify the molecular features that predict the response to DAC (24-26).

The present study investigated the mechanisms of DAC-induced demethylation and expression restoration of tumor suppressor genes via studies in the MDS-derived leukemic cell line MDS-L (27).

Materials and methods

Chemicals and reagents. DAC was purchased from Sigma-Aldrich (Merck KGaA). MDS-L cells, a blastic subline derived from bone marrow blasts isolated from a 50-year-old male Japanese patient with MDS that was established in a previous study (27), were used in the present study. The cells were cultured in RPMI 1640 (FUJIFILM Wako Pure Chemical Corporation) medium supplemented with 20% heat-inactivated fetal bovine serum (FUJIFILM Wako Pure Chemical Corporation) and maintained in a humidified atmosphere with 5% CO_2 at 37˚C. The cells were cultured with a non-toxic concentration (5 nM) of DAC at 37˚C for 96 h and passaged for 6 months to generate the MDS-L-DAC cell line.

Cell line characteristics. A proliferation assay was performed using the trypan dye exclusion method to determine the effects of DAC on growth inhibition during 72 h of treatment. The cell suspension and 0.5 % trypan blue staining solution (Nacalai Tesque, Inc.) were mixed in a 1:3 ratio at room temperature for 5 min and the number of live cells was measured using a hemocytometer under a light microscope. The IC_{50} values were calculated from the growth inhibition curves generated with GraphPad Prism software (version 8.0; Dotmatics).

Cellular morphology was investigated using May-Grunwald-Giemsa staining. Using 100 μl of cell culture ($2x10^6$ cells/ml), samples were centrifuged in a cytospin at 60 x g for 2 min at 4˚C. May-Grunwald's stain solution (Nakalai Tesque, Inc.) was diluted two-fold with 100% methanol and added to the specimens, which were then fixed and stained at room temperature for 5 min. Giemsa's stain solution was diluted 20-fold with M/15 phosphate buffer (pH 7.4) (Muto Pure Chemicals Co., Ltd.) added to the preparation, and stained at room temperature for 20 min. Specimens were observed using a light microscope (BX51; Oly) and images were captured using cellSens Standard software (version 1.16; Evident Scientific).

Cell surface markers were detected by SRL, Inc. (H.U. Group Holdings, Inc.). Cells ($5x10^5$ cells) were collected and aliquoted for flow cytometric analysis and were incubated with fluorochrome-conjugated monoclonal antibodies against the indicated surface makers for 25 min at room temperature in the dark. Following antibody staining, PBS was added to the samples, which were then gently mixed and incubated for 7 min at room temperature. After incubation, cells were washed using centrifugation at 4˚C at 620 x g for 5 min, and the supernatant was discarded. The cell pellets were then resuspended in cold PBS and analyzed using fluorescence-activated cell sorting FACSCanto™ II flow cytometry (BD Biosciences). Data acquisition was carried out using FACSDiva™ software (version 6.1.3; BD Biosciences) and leukocyte populations were identified based on the expression of CD45. The expression of surface markers was identified using the following antibodies: CD11b (cat. no. 347557; 1:20), CD15 (cat. no. 567961; 1:20), CD13 (cat. no. 565124; 1:20), CD19 (cat. no. 562441; 1:20), CD33 (cat. no. 572166; 1:20), glycophorin A (expressed in erythrocyte progenitor cells and erythrocytes) (cat. no. 561775; 1:20), CD7 (cat. no. 659124; 1:20), CD34 (cat. no. 659123; 1:20), CD10 (cat. no. 563508; 1:20) and HLA-DR (cat. no. 569674; 1:20) all obtained from BD Biosciences antigen was evaluated. The activity of DNMT was measured using a DNMT assay kit according to the manufacturer's protocol (Active Motif, Inc.).

DNA methylation array analysis. DNA was extracted from cells using a QIAamp DNA Mini kit (Qiagen Sciences, Inc.). All DNA samples were quantified using the fluorometric method and assessed for purity with a NanoDrop2000c (Thermo Fisher Scientific, Inc.). DNA methylation array analysis was performed using the Infinium Human Methylation 450 BeadChip (Illumina, Inc.) and included evaluation of DNA methylation at 485,576 CpG sites. The BeadChips were scanned using an Illumina HiScan SQ scanner. The intensities of the images were extracted using GenomeStudio (version 2010.3) and Methylation module (version 1.8.5) software (Illumina, Inc.). Hierarchical clustering of differentially methylated genomic regions was performed using RnBeads (version 2.14.0; https://rnbeads.org/) for MDS-L and MDS-L-DAC cells using the 100 genes and promoters identified with the most significant methylation changes.

Reverse transcription (RT)-PCR. RNA was extracted from cells using a RNeasy Mini Kit (Qiagen Sciences, Inc.). Total RNA was reverse transcribed to cDNA using a PrimeScript™ RT-PCR kit (Takara Bio, Inc.) and TaqMan™ MicroRNA Reverse Transcription kit (cat. no. 4366597; Thermo Fisher Scientific, Inc.). Quantitative PCR was carried out using a TaqMan Fast Advanced Master Mix kit and Step One Plus real-time PCR systems (Applied Biosystems; Thermo Fisher Scientific, Inc.) with the following conditions: An initial 95˚C for 20 sec, followed by 40 cycles of 95˚C for 1 sec and 60˚C for 20 sec. The transcript levels of Wilms' tumor 1 (WT1) were measured via RT-PCR with the Otsuka WT1 mRNA OneStep Assay (WT1, Hs01103751_m1; Thermo Fisher Scientific, Inc.) according to the manufacturer's protocol. The expression levels of membrane spanning 4-domains A3 (MS4A3), KRAS and miR143 were measured using TaqMan® Gene Expression Assays (Applied Biosystems™; Thermo Fisher Scientific, Inc.). The expression levels were evaluated using the $2^{-\Delta\Delta Cq}$ method (28). Assay IDs used were as follows: MS4A3, ID no. Hs00960994_m1; KRAS, ID no. Hs00364284_g; GAPDH, ID no. Hs02786624_g1; hsa-miR-143, ID no. 477912_mir (miR-143 sequence, 5'-UGAGAUGAAGCACUGUAGCUC-3'); and U6 snRNA, ID no. 001973 (Applied Biosystems™; Thermo Fisher Scientific, Inc.), respectively.

Western blot analysis. Western blot analysis was performed to measure the protein expression levels of demethylation genes. After culturing the cells at 37˚C for 48 h, theses were washed with PBS, and protein lysates were extracted from the cells

($1x10^7$ cells) using the Qproteome Mammalian Protein Prep kit (Qiagen, Inc.). Protein quantification was carried out using the BCA method. The 20 μg lysates were electrophoresed in a 10-20% e-PAGEL gel (ATTO Corporation) and were and transferred onto a Immun-Blot PVDF Membrane for Protein Blotting (Bio-Rad Laboratories, Inc.). Blocking was carried out using an undiluted solution of Blocking One (Nacalai Tesque, Inc.) and incubated at room temperature for 30 min. The membranes were probed with primary antibodies overnight at 4˚C and the membrane was washed with TBST containing 0.001% Tween20. Subsequently, the membrane was probed with secondary antibodies for 1 h at room temperature and the membrane was washed with TBST containing 0.01% Tween20. Western lighting ECL Pro (PerkinElmer, Inc.) and FUSION-SOLO.7S. EDGE (Vilber Lourmat) were used to visualize and quantify protein signals. Mouse polyclonal anti-MS4A3 antibody (cat. no. ab68207; 1:500; Abcam) was used as a primary antibody. The primary antibodies caspase 3 (cat. no. 9662; 1:1,000), cleaved caspase 3 (cat. no. 9661; 1:1,000), caspase 8 (cat. no. 9746; 1:1,000), cleaved caspase 3 (cat. no. 9496; 1:1,000), heat shock protein 70 (Hsp70; cat. no. 4872; 1:1,000) and β-actin (cat. no. 3700 1:1,000) were from Cell Signaling Technology, Inc. The Bcl-2 antibody (cat. no. ab182858; 1:1,000) was from Abcam and heat shock protein 90 (Hsp90; cat. no. AC88; 1:1,000) was from Enzo Life Sciences, Inc. The secondary antibody used was either, Peroxidase AffiniPure Goat Anti-Rabbit IgG (cat. no. 111-035-144; 1:10,000) or Peroxidase-AffiniPure Goat Anti-Mouse IgG, F(ab')2 Fragment Specific (cat. no. 115-035-072; 1:10,000) from Jackson ImmunoResearch Laboratories, Inc. Band density was detected using a FUSION-SOLO.7S.EDGE (Vilber Lourmat). Unpaired Student's t tests were carried out using GraphPad Prism software (version 5.0; Dotmatics). One-way analysis of variance followed by Tukey's test was used to compare multiple groups.

Apoptosis rate by cell cycle. Cells ($5x10^5$ cells) were washed with PBS. The mixture was centrifuged at 4˚C at 200 x g for 5 min before the supernatant was removed and ice-cold 70% methanol was added to the cell pellet and then incubated on ice for 30 min. The mixture was centrifuged again at 4˚C at 400 x g for 5 min, and the supernatant was removed and the cell pellet was resuspended in PBS. Subsequently, 10 mg/ml RNnase A solution (Sigma-Aldrich; Merck KGaA) was added and incubated at 37˚C for 20 min. The mixture was centrifuged at 4˚C at 400 x g for 5 min, and the supernatant was removed and the cell pellet was resuspended in PBS. Subsequently, 500 μg/ml PI solution (Nacalai Tesque, Inc.) was added and the cells were incubated on ice for 20 min. Analysis was carried out using a FACSCanto™ II flow cytometer (BD Biosciences). Unstained cells and isotype controls were used to set up background fluorescence and gating. Cells were first gated using forward scatter. The main cell population was then analyzed. Data analysis was carried out using BD FACSDiva™ software (version 6.1.3; BD Biosciences).

Quantification of β-catenin positivity. The percentage of β-catenin positive cells was determined using flow cytometry and the primary anti-β-catenin antibody (cat. no. 8480; 1:50; Cell Signaling Technology, Inc.) and a secondary antibody anti-rabbit IgG (H+L), F(ab')2 Fragment (Alexa Fluor® 488 conjugate) (cat. no. 4412; 1:250; Cell Signaling Technology, Inc.). Cells ($1x10^6$ cells) were washed with PBS and after centrifugation at 200 x g for 5 min at 4˚C, the supernatant was removed and fixed with 4% formaldehyde for 10 min at 37˚C. The sample was centrifuged at 200 x g for 5 min at 4˚C, and the fixative was removed. Then, ice-cold 90% methanol was added and incubated on ice for 30 min. The mixture was centrifuged at 200 x g and 4˚C for 5 min, and the permeate was removed. The cells were washed with PBS, and the mixture was centrifuged at 200 x g for 5 min at 4˚C to remove the supernatant. The anti-β-catenin antibody was added and incubated at room temperature for 1 h. The cells were washed with PBS, and the mixture was centrifuged at 200 x g for 5 min at 4˚C to remove the supernatant. The secondary antibody was added and incubated at room temperature for 30 min. The cells were washed with PBS and the mixture was centrifuged at 200 x g for 5 min at 4˚C to remove the supernatant. This was resuspended in PBS and was then analyzed using a FACSCanto™ II flow cytometer (BD Biosciences). Unstained cells and isotype controls were used to set up background fluorescence and gating. Cells were first gated using forward scatter. The main cell population was then analyzed. Data analysis was carried out using BD FACSDiva™ software (version 6.1.3; BD Biosciences).

Statistical analyses. All statistical analyses were performed using Microsoft Excel (Microsoft Corporation). The unpaired Student's t-test was conducted to compare the differences between two groups. One-way analysis of variance followed by Tukey's test was used to compare multiple groups. All graphs, linear regression lines and curves were generated using the GraphPad Prism software (version 8.0; Dotmatics). $P<0.05$ was considered to indicate a statistically significant difference.

Results

DAC induces the differentiation of MDS-L cells. The IC_{50} value of DAC in MDS-L cells was 64 nM (Fig. S1). As the efficacy of DAC is most notable in patients with MDS after the fourth cycle of 6-weekly dosing (6 months) in clinical practice, MDS-L cells were incubated with a 5 nM of DAC, the lowest concentration that could inhibit DNMT activity without inducing cytotoxicity, for 6 months, which generated the MDS-L-DAC cell line. Compared with that in the parental MDS-L cells, the enzymatic activity of DNMT1 in MDS-L-DAC cells was significantly inhibited by DAC treatment (Fig. 1A). There was no significant difference in the ability of DAC incorporation into cellular DNA between the MDS-L and MDS-L-DAC cells (Fig. 1B). Morphologically, the MDS-L-DAC cells were mature and differentiated, with lobulated nuclei and cytoplasmic granulation (Fig. 1C). Compared with the MDS-L cells, the MDS-L-DAC cells had a significantly reduced positivity for CD34 and MHC class II DR antigen, and an increased positivity for CD15 (Figs. 1D and S2) and partial loss of chromosomal abnormalities (Fig. S3).

Profiling of DNA demethylation upon DAC exposure. Comprehensive genome-wide profiling of DNA methylation in MDS-L and MDS-L-DAC cells was performed to investigate

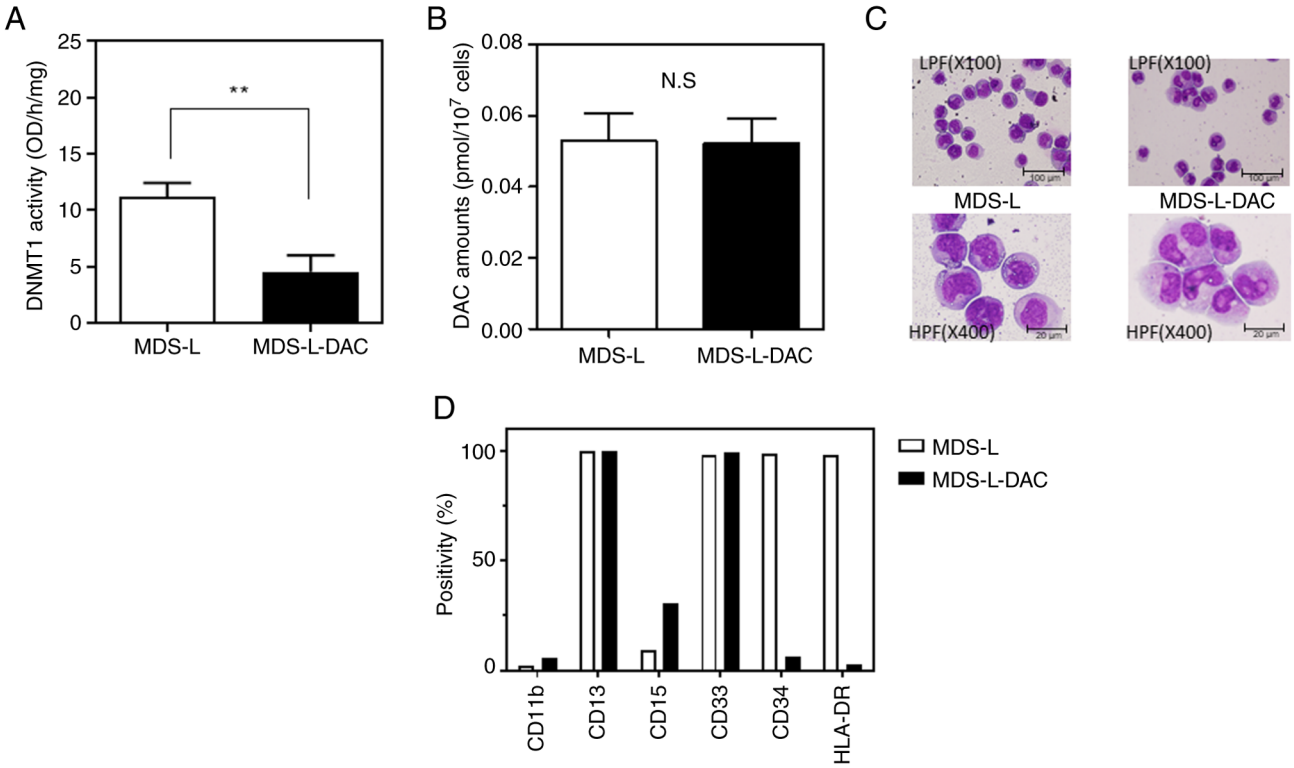

Figure 1. DAC induces the differentiation of MDS-L cells. (A) The enzymatic activity of DNMT1 was measured in both MDS-L and cell lines. MDS-L 11.17±1.25; MDS-L-DAC 4.55±1.46, P=0.004, using Student's t-test. (B) Incorporation of DAC into the DNA of MDS-L cells and MDS-L-DAC cells. Data shown as mean ± SD of ≥3 independent experiments. (C) Morphological changes in MDS-L and MDS-L-DAC cells observed by May-Grunwald Giemsa staining. Upper panel (scale bar, 100 μm): 100-fold of MDS-L cells (left) and MDS-L-DAC cells (right). Lower panel (scale bar, 20 μm): 400-fold of MDS-L cells (left) and MDS-L-DAC cells (right). (D) Flow cytometric analysis of CD11b, CD13, CD15, CD33, CD34 and HLA-DR expression. **P<0.01. DNMT1, DNA methyltransferase 1; MDS, myelodysplastic syndromes; MDS-L, MDS cell line; DAC, decitabine; N.S., not significant; HLA-DR, MHC class II DR antigen.

the epigenetic changes induced by DAC in MDS-L cells. Clustering analysis was performed on the 100 CpG sites, CpG islands, tiling regions (evaluated over a large region containing up to 5,000 bp), genes and promoters with the greatest differences in β values between MDS-L and MDS-L-DAC cells. DAC treatment resulted in the demethylation of 80 CpG sites and 79 tiling regions (Fig. S4). Regarding gene regions and promoter regions with methylation changes, 75 gene regions and 76 promoter regions were demethylated in MDS-L-DAC cells (Fig. 2A and B). Among these gene regions and promoter regions, excluding pseudogenes and long non-coding RNAs, 24 gene regions and 35 promoter regions were found to exhibit significant demethylation (Tables SI and SII).

Restoration of MS4A3 expression and induction of apoptosis in MDS-L-DAC cells. In MDS-L-DAC cells, increased expression levels of MS4A3 were observed at both the transcriptional and translational levels (Fig. 3A and B). DAC treatment induced apoptosis in 20% of the MDS-L-DAC cells, compared with only 5% of the control MDS-L cells (Figs. 3C and S5). Additionally, 20% of cells treated with 50 nM decitabine underwent apoptosis, compared with only 10% of the control cells, accompanied by markedly increased cleavage of caspase-3 and caspase-8 (Fig. 3D), compared with that of MDS-L cells, which suggested the involvement of MS4A3-mediated apoptosis (29). Expression of MS4A3 is also known to induce cell differentiation (30), and the induction of differentiation in MDS-L-DAC cells as aforementioned also suggested the restoration of MS4A3 expression.

Upregulation of miR143 in MDS-L-DAC cells. The expression of miR143 significantly increased in MDS-L-DAC cells compared with that of MDS-L cells, consistent with the DNA methylation profile (Fig. 4A). miR143 expression is typically downregulated in hematopoietic malignancies (30), thus, changes in the expression levels of molecules downstream of the restored miR143 expression in MDS-L-DAC cells were examined. The expression levels of KRAS and WT1, which are components of the downstream signaling pathways of miR143 (31,32), were significantly decreased in MDS-L-DAC cells compared with that of MDS-L cells (Fig. 4B). In addition, MDS-L-DAC cells presented decreased expression levels of β-catenin, Bcl-2, Hsp70 and Hsp90 (Fig. 4C and D; Fig. S6), which suggested a decrease in leukemogenicity due to the restoration of miR143 expression.

Discussion

DAC is an effective HMA used for the treatment of MDS and AML (5,24). However, in contrast to other cytotoxic agents such as hydroxycarbamide and cytarabine, the mechanism underlying the demethylation effect of DAC remains unclear. Since DAC is rapidly eliminated by the enzyme cytidine deaminase, with a half-life of <20 min *in vivo* and 5-16 h *in vitro* (33),

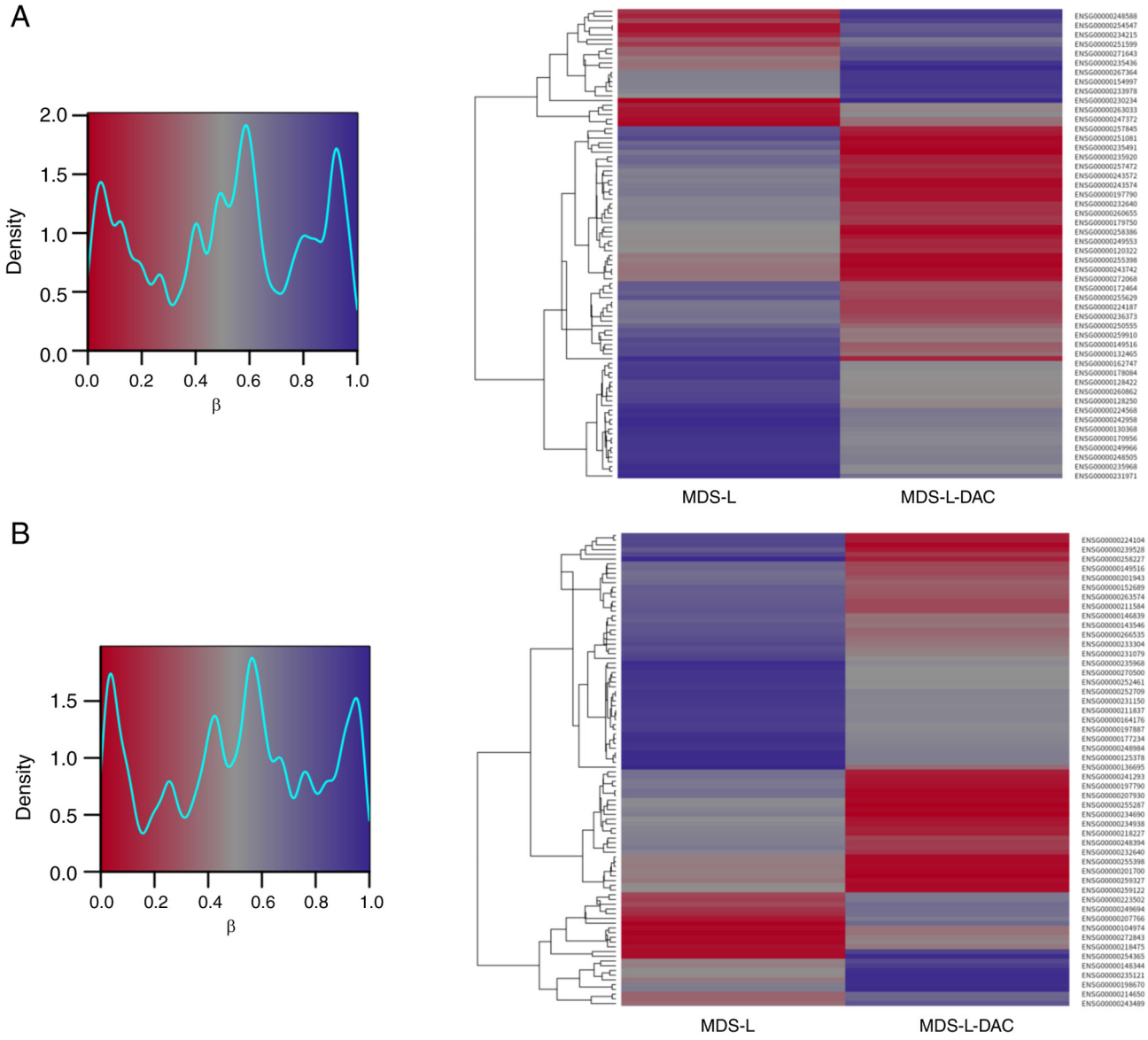

Figure 2. DNA methylation array analysis. Hierarchical clustering of differentially methylated genomic regions in MDS-L and MDS-L-DAC cells on the basis of the 100 genes and promoters with the most significant methylation changes. A gradient color scale ranging between blue (completely unmethylated) to red (completely methylated) is shown. (A) Genes and (B) promoters. MDS, myelodysplastic syndromes; MDS-L, MDS cell line; DAC, decitabine.

the present study explored the genes involved in the DAC response in MDS-L cells with long-term exposure to DAC. In MDS-L cells, long-term culture with DAC significantly reduced DNMT1 activity and altered the methylation profiles of multiple genes, including MS4A3 and miR143, leading to cell differentiation and gene expression. These results may suggest a mechanism for HMA-induced expression recovery and differentiation in MDS-L cells.

DNA methylation array analysis was used to evaluate the methylation status of CpG sites, CpG islands, tiling regions, promoter regions and gene regions in MDS-L and MDS-L-DAC cells, which were compared to assess methylation changes comprehensively. In MDS-L-DAC cells, demethylation of both MS4A3 and miR143 was observed, further confirming the restoration of the expression of these genes. Among them, MS4A3 is a member of the MS4 protein family, whose members possess four transmembrane domains, and are known to function as cell surface signaling receptors and intracellular adapter proteins (34). MS4A3 is expressed in specific subsets of hematopoietic cells, including myeloid precursors, basophilic granulocytes and CD34-positive hematopoietic stem and progenitor cells (30,34,35). Increased expression levels of MS4A3 in hematopoietic stem cells induces differentiation into granulocytes (30); conversely, suppression of MS4A3 in AML cells is involved in tumor aggressiveness (29). In MDS-L-DAC cells, a tendency toward differentiation and the induction of apoptosis were observed, which may involve the restoration of MS4A3 expression levels. The present study was not able to validate this observation due to the lack of other MDS cell lines for examination; thus, a limitation is that the present findings were exclusively observed in MDS-L cells. Future work is necessary to validate the restoration of MS4A3 expression levels and therapeutic effects in cells derived from patients with MDS.

MicroRNA-143 is known to serve important roles in cell proliferation, cell death and metastasis in various types of cancer, including AML, osteosarcoma and bladder cancer,

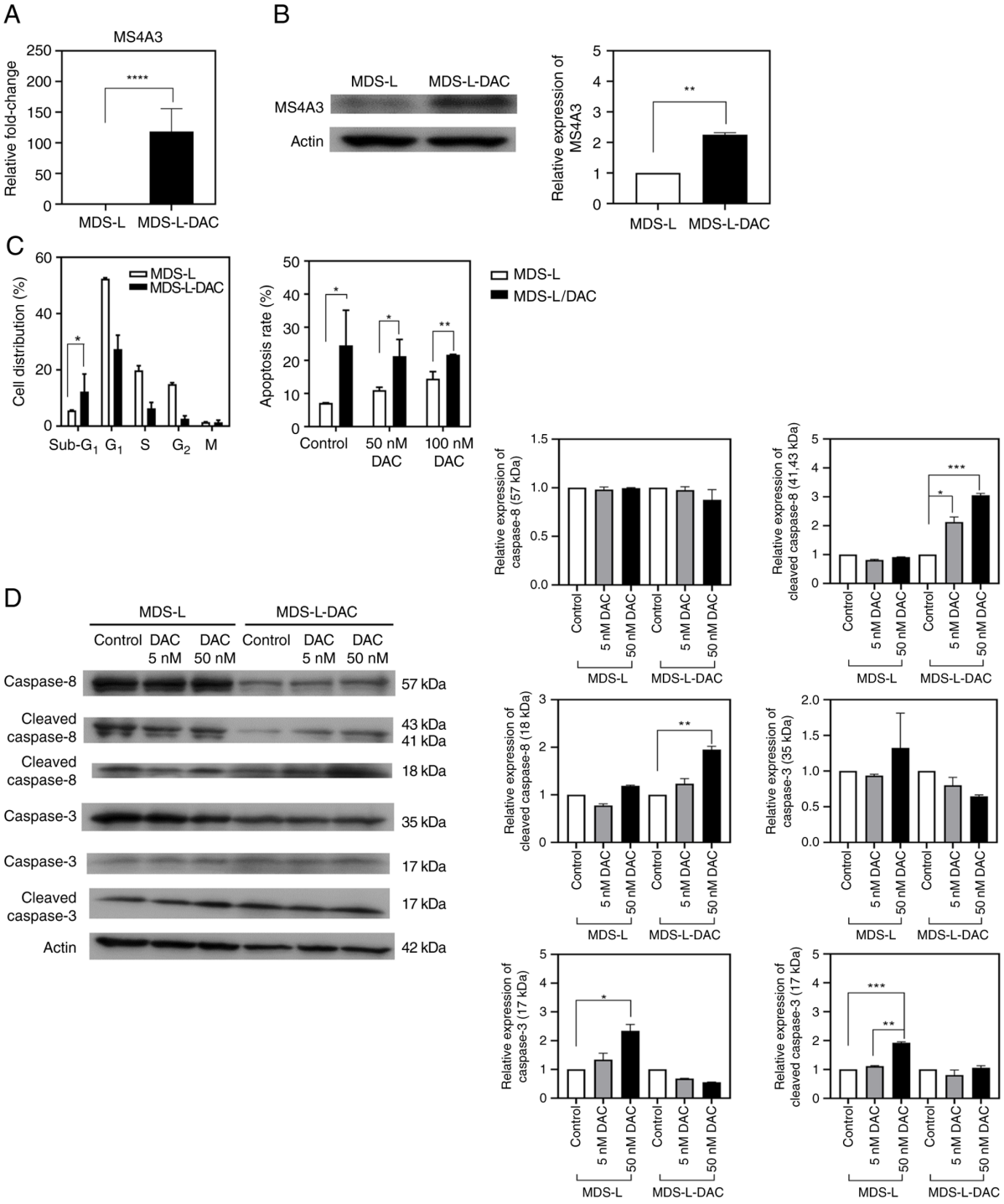

Figure 3. Restoration of MS4A3 expression levels and induction of apoptosis in MDS-L-DAC cells. (A) Reverse transcription-quantitative PCR was performed to evaluate the expression of MS4A3. Relative expression value of MDS-L-DAC was 118±37.3 compared with the MDS-L group. (B) Western blot analysis was performed to evaluate the protein level of MS4A3. (C) Percentages of apoptotic cells treated with various concentrations of DAC. The proportions of sub-G_1 group of each were 5.6±0.14 in MDS-L and 12.3±6.25 in MDS-L-DAC groups (P=0.04, Student's t-test). The proportion of apoptotic cells was 7.13±0.06 in MDS-L and 24.5±10.6 in MDS-L-DAC in the control groups, 11.0±0.86 and 21.3±5.06 when treated with 50 nM DAC, and 14.5±2.15 and 21.7±0.1 when treated with 100 nM DAC, respectively. Statistical analysis was performed using Student's t-test. (D) Western blot analysis was carried out to evaluate the protein levels of caspase 3, cleaved caspase 3, caspase 8 and cleaved caspase 8. *P<0.05, **P<0.01, ***P<0.001 and ****P<0.0001. MDS, myelodysplastic syndromes; MDS-L, MDS cell line; DAC, decitabine; MS4A3, membrane spanning 4-domains A3.

and is known to function as a tumor suppressor (36-39). In the present study, a decrease in the expression levels of KRAS and WT1, as well as in the downstream signaling molecules β-catenin and Hsp70, were observed in MDS-L-DAC cells. In colon cancer cells, miR143 has been shown to bind to the 3'-untranslated region of the KRAS and inhibit KRAS expression (31). It has also been shown that TGF-β1-mediated induction of miR143 reduces WT1 expression levels in human podocytes (32). Through these mechanisms, the restoration of miR143 expression levels in MDS-L-DAC cells may have

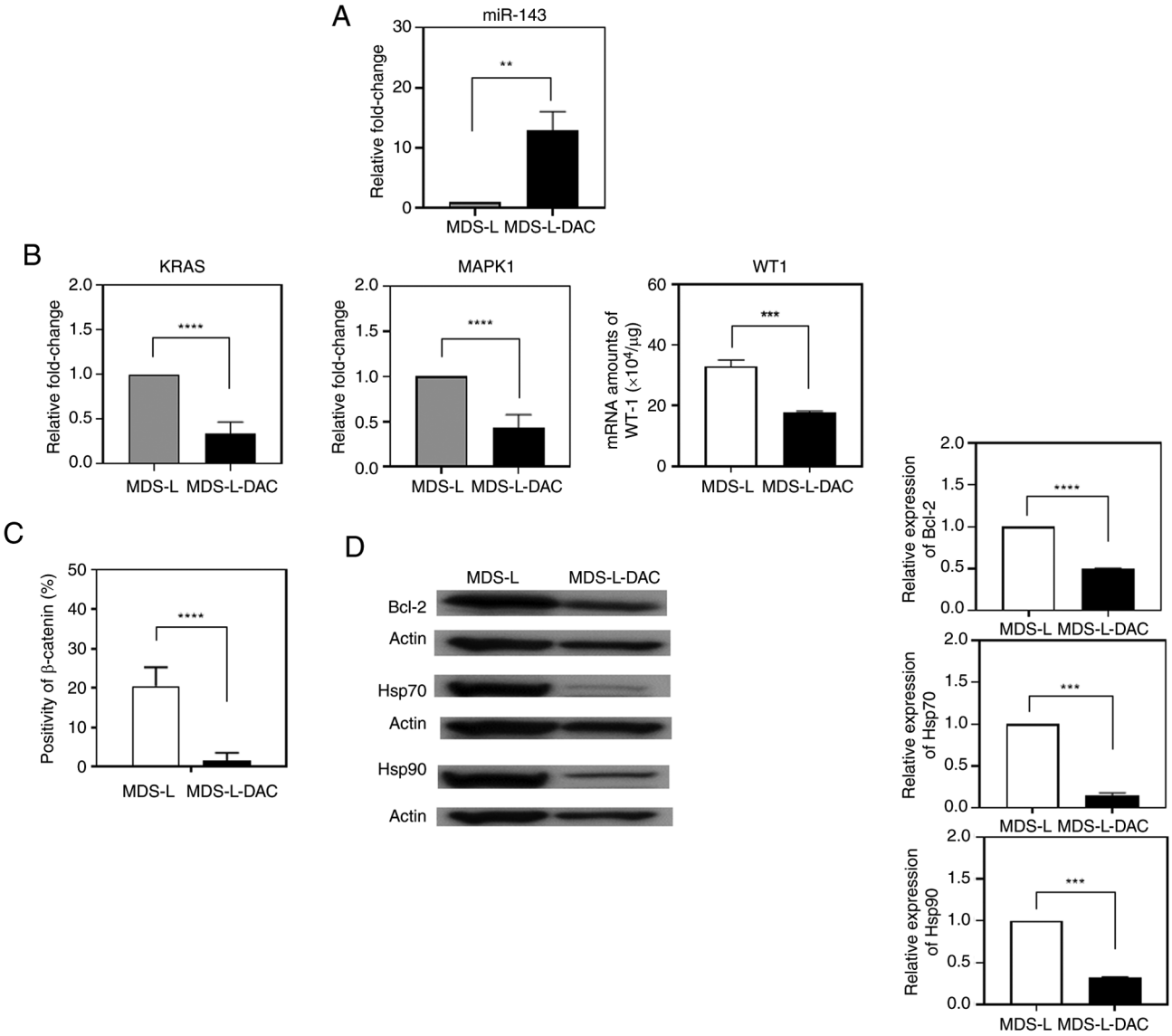

Figure 4. Upregulation of miR143 in MDS-L-DAC cells. (A) RT-PCR was performed to evaluate the expression of miR143. Relative expression value of MDS-L-DAC was 6.96±2.67 compared with the MDS-L group. Statistical analysis was performed using Student's t-test. (B) RT-PCR was performed to evaluate the expression of KRAS, MAPK1 and WT1. Relative expression value of MDS-L-DAC was 0.33±0.14 in KRAS and 0.43±0.15 in MAPK1 compared with the MDS-L group. Expression of WT1 mRNA was 33.0±2.0 in MDS-L and 17.7±0.58 in MDS-L-DAC. Statistical analysis was performed using Student's t-test. (C) The expression of β-catenin was evaluated using flow cytometry. The proportions of β-catenin positivity were 20.5±4.79 in MDS-L and 1.64±1.90 in the MDS-L-DAC group. Statistical analysis was performed using Student's t-test. (D) Western blot analysis was performed to evaluate the protein levels of Bcl-2, Hsp70 and Hsp90. **P<0.01, ***P<0.001 and ****P<0.0001. MDS, myelodysplastic syndromes; MDS-L, MDS cell line; DAC, decitabine; Hsp, heat shock protein; RT, reverse transcription; miR, microRNA; WT, Wilms tumor 1.

reduced WT1 expression levels. Furthermore, by evaluating molecules downstream of miR143 and WT1 (40), Hsp70 and β-catenin were downregulated in MDS-L-DAC cells, compared with that of MDS-L cells. The expression levels of Bcl-2 and Hsp90, key molecules of WT1 signaling were evaluated, and it was found Bcl-2 and Hsp90 expression levels were also decreased in MDS-L-DAC cells. Upregulation of Hsp70 and β-catenin is associated with a poor therapeutic response and adverse prognosis in AML (41,42), and therefore, decreased expression of these predictors of adverse outcomes in MDS-L-DAC cells potentially indicated that hsp70 and β-catenin may be future therapeutic targets via miR143. In addition to these changes in gene expression, it is suggested that exposure to DAC may cause the demethylation of genes, such as *CDNK2B* and *TP73* (43,44), which may be involved in cell differentiation. Further evaluation using patient samples derived from MDS may clarify this point in the future.

In conclusion, the expression of MS4A3 and miR143 was epigenetically silenced in the MDS-L cell line, and long-term culture of the MDS-L cell line with DAC resulted in the restoration of MS4A3 and miR143 expression. As a result, the restoration of MS4A3 expression, along with suppression of the expression of KRAS, WT1 and Wnt/β-catenin pathway components downstream of miR143, induced cell differentiation and apoptosis was induced. The changes in methylation profiles upon long-term DAC treatment suggest that the MS4A3 and miR143 genes and their downstream signaling pathways may be potential therapeutic targets in AML in the future.

Acknowledgements

The authors would like to thank Mr. Daisuke Minegishi of Tohoku Chemical Co., Ltd., (Iwate, Japan) for his guidance in DNA methylation array analysis.

Funding

The present work was supported in part by a Grant-in-Aid for Scientific Research from the Ministry of Education, Culture, KAKENHI (grant nos. 23501307 and 19K07637), the NAITO foundation (grant no. 20-007) and a grant from Japan Gout Research Foundation (2008, 2009 and 2010).

Availability of data and materials

The data generated in the present study may be found in the National Center for Biotechnology Information Gene Expression Omnibus database under the accession no. GSE293053 or at the following URL: https://www.ncbi.nlm.nih.gov/geo/query/acc.cgi?acc=GSE293053.

Authors' contributions

NH and TY designed and conducted the present study. RN carried out the high-throughput sequencing experiments and performed the examination of flow cytometry, PCR and western blotting. NH, RN and TY analyzed the experimental results and considered and conducted necessary additional experiments. RN and NH contributed to manuscript writing. KT generated the MDS-L cell lines. NH and TY confirm the authenticity of all the raw data. All authors read and approved the final version of the manuscript.

Ethics approval and consent to participate

Not applicable.

Patient consent for publication

Not applicable.

Competing interests

The authors declare that they have no competing interests.

References

1. National Cancer Institute, Surveillance, Epidemiology, and End Results Program: SEER*Explorer: An interactive website for SEER cancer statistics. https://seer.cancer.gov/statistics-network/explorer/application.html. Accessed August 20, 2026.
2. Sekeres MA, Schoonen WM, Kantarjian H, List A, Fryzek J, Paquette R and Maciejewski JP: Characteristics of US patients with myelodysplastic syndromes: Results of six cross-sectional physician surveys. J Natl Cancer Inst 100: 1542-1551, 2008.
3. Lin RJ and Artz AS: Allogeneic hematopoietic cell transplantation for older patients. Hematology Am Soc Hematol Educ Program 2021: 254-263, 2021.
4. Silverman LR, Fenaux P, Mufti GJ, Santini V, Hellström-Lindberg E, Gattermann N, Sanz G, List AF, Gore SD and Seymour JF: Continued azacitidine therapy beyond time of first response improves quality of response in patients with higher-risk myelodysplastic syndromes. Cancer 117: 2697-2702, 2011.
5. Lübbert M, Suciu S, Baila L, Rüter BH, Platzbecker U, Giagounidis A, Selleslag D, Labar B, Germing U, Salih HR, *et al*: Low-dose decitabine versus best supportive care in elderly patients with intermediate- or high-risk myelodysplastic syndrome (MDS) ineligible for intensive chemotherapy: Final results of the randomized phase III study of the European Organisation for Research and Treatment of Cancer Leukemia Group and the German MDS Study Group. J Clin Oncol 29: 1987-1996, 2011.
6. Christman JK: 5-Azacytidine and 5-aza-2'-deoxycytidine as inhibitors of DNA methylation: Mechanistic studies and their implications for cancer therapy. Oncogene 21: 5483-5495, 2002.
7. Castillo-Aguilera O, Depreux P, Halby L, Arimondo PB and Goossens L: DNA methylation targeting: The DNMT/HMT crosstalk challenge. Biomolecules 7: 3, 2017.
8. Willemze R, Suciu S, Archimbaud E, Muus P, Stryckmans P, Louwagie EA, Berneman Z, Tjean M, Wijermans P, Dohner H, *et al*: A randomized phase II study on the effects of 5-Aza-2'-deoxycytidine combined with either amsacrine or idarubicin in patients with relapsed acute leukemia: An EORTC Leukemia Cooperative Group phase II study (06893). Leukemia 11 (Suppl): S24-S27, 1997.
9. Jones PA and Taylor SM: Cellular differentiation, cytidine analogs and DNA methylation. Cell 20: 85-93, 1980.
10. Momparler RL: Pharmacology of 5-Aza-2'-deoxycytidine (decitabine). Semin Hematol 42 (Suppl): S9-S16, 2005.
11. Baylin SB: DNA methylation and gene silencing in cancer. Nat Clin Pract Oncol 1 (Suppl): S4-S11, 2005.
12. Herman JG and Baylin SB: Gene silencing in cancer in association with promoter hypermethylation. N Engl J Med 349: 2042-2054, 2003.
13. Leone G, Teofili L, Voso MT and Lübbert M: DNA methylation and demethylating drugs in myelodysplastic syndromes and secondary leukemias. Haematologica 87: 1324-1341, 2002.
14. Riyas Mohamed FR, Aldubaisi S, Akbar A, Khan MI and Yaqinuddin A: Epigenetic reprogramming by decitabine in triple-negative breast cancer: Mechanisms, immune modulation, and therapeutic synergy. Cancers (Basel) 17: 2953, 2025.
15. Zeng W, Dai H, Yan M, Cai X, Luo H, Ke M and Liu Z: Decitabine-induced changes in human myelodysplastic syndrome cell line SKM-1 are mediated by FOXO3A activation. J Immunol Res 2017: 4302320, 2017.
16. Cardoso C, Pestana D, Gokuladhas S, Marreiros AD, O'Sullivan JM, Binnie A, TFernandes M and Castelo-Branco P: Identification of novel DNA methylation prognostic biomarkers for AML with normal cytogenetics. JCO Clin Cancer Inform 8: e2300265, 2024.
17. Dexheimer GM, Alves J, Reckziegel L, Lazzaretti G and Abujamra AL: DNA methylation events as markers for diagnosis and management of acute myeloid leukemia and myelodysplastic syndrome. Dis Markers 2017: 5472893, 2017.
18. Metzeler KH, Walker A, Geyer S, Garzon R, Klisovic RB, Bloomfield CD, Blum W and Marcucci G: DNMT3A mutations and response to the hypomethylating agent decitabine in acute myeloid leukemia. Leukemia 26: 1106-1107, 2011.
19. Ley TJ, Ding L, Walter MJ, McLellan MD, Lamprecht T, Larson DE, Kandoth C, Payton JE, Baty J, Welch J, *et al*: DNMT3A mutations in acute myeloid leukemia. N Engl J Med 363: 2424-2433, 2010.
20. Casellas Roman HL, Venugopal K, Feng Y, Shabashvili DE, Posada LM, Li J and Guryanova OA: DNMT3A alterations associated with myeloid malignancies dictate differential responses to hypomethylating agents. Leuk Res 94: 106372, 2020.
21. Blum W, Garzon R, Klisovic RB, Schwind S, Walker A, Geyer S, Liu S, Havelange V, Becker H, Schaaf L, *et al*: Clinical response and miR-29b predictive significance in older AML patients treated with a 10-day schedule of decitabine. Proc Natl Acad Sci USA 107: 7473-7478, 2010.
22. Mims A, Walker AR, Huang X, Sun J, Wang H, Santhanam R, Dorrance AM, Walker C, Hoellerbauer P, Tarighat SS, *et al*: Increased anti-leukemic activity of decitabine via AR-42-induced upregulation of miR-29b: A novel epigenetic-targeting approach in acute myeloid leukemia. Leukemia 27: 871-878, 2013.
23. Yang H, Fang Z, Wei Y, Hu Y, Calin GA, Kantarjian HM and Garcia-Manero G: Levels of miR-29b do not predict for response in patients with acute myelogenous leukemia treated with the combination of 5-azacytidine, valproic acid, and ATRA. Am J Hematol 86: 237-238, 2011.

24. Welch JS, Petti AA, Miller CA, Fronick CC, O'Laughlin M, Fulton RS, Wilson RK, Baty JD, Duncavage EJ, Tandon B, *et al*: TP53 and decitabine in acute myeloid leukemia and myelodysplastic syndromes. N Engl J Med 375: 2023-2036, 2016.
25. Meldi K, Qin T, Buchi F, Droin N, Sotzen J, Micol JB, Selimoglu-Buet D, Masala E, Allione B, Gioia D, *et al*: Specific molecular signatures predict decitabine response in chronic myelomonocytic leukemia. J Clin Invest 125: 1857-1872, 2015.
26. Kim S, Shin DY, Kim D, Oh S, Hong J, Kim I and Kim E: Gene expression profiles identify biomarkers of resistance to decitabine in myelodysplastic syndromes. Cells 10: 3494, 2021.
27. Tohyama K, Tsutani H, Ueda T, Nakamura T and Yoshida Y: Establishment and characterization of a novel myeloid cell line from the bone marrow of a patient with the myelodysplastic syndrome. Br J Haematol 87: 235-242, 1994.
28. Livak KJ and Schmittgen TD: Analysis of relative gene expression data using real-time quantitative PCR and the 2-DDct method. Methods 25: 402-408, 2001.
29. Heller G, Rommer A, Steinleitner K, Etzler J, Hackl H, Heffeter P, Tomasich E, Filipits M, Steinmetz B, Topakian T, *et al*: EVI1 promotes tumor growth via transcriptional repression of MS4A3. J Hematol Oncol 8: 28, 2015.
30. Donato JL, Ko J, Kutok JL, Cheng T, Shirakawa T, Mao XQ, Beach D, Scadden DT, Sayegh MH and Adra CN: Human HTm4 is a hematopoietic cell cycle regulator. J Clin Invest 109: 51-58, 2002.
31. Chen X, Guo X, Zhang H, Xiang Y, Chen J, Yin Y, Cai X, Wang K, Wang G, Ba Y, *et al*: Role of miR-143 targeting KRAS in colorectal tumorigenesis. Oncogene 28: 1385-1392, 2009.
32. Tabei A, Sakairi T, Hamatani H, Ohishi Y, Watanabe M, Nakasatomi M, Ikeuchi H, Kaneko Y, Kopp JB and Hiromura K: The miR-143/145 cluster induced by TGF-beta1 suppresses Wilms' tumor 1 expression in cultured human podocytes. Am J Physiol Renal Physiol 325: F121-F133. 2023.
33. Derissen EJ, Beijnen JH and Schellens JH: Concise drug review: Azacitidine and decitabine. Oncologist 18: 619-624, 2013.
34. Kutok JL, Yang X, Folkerth R and Adra CN: Characterization of the expression of HTm4 (MS4A3), a cell cycle regulator, in human peripheral blood cells and normal and malignant tissues. J Cell Mol Med 15: 86-93, 2011.
35. Kutok JL, Yang X, Folkerth RD, Imitola J, Raddassi K, Yano Y, Salahuddin S, Lawitts J, Imboden H, Chinami M, *et al*: The cell cycle associated protein, HTm4, is expressed in differentiating cells of the hematopoietic and central nervous system in mice. J Mol Histol 36: 77-87, 2005.
36. Li F, Han Y, Chen R, Jiang Y, Chen C, Wang X, Zhou J, Xu Q, Jiang S, Zhang S, *et al*: MicroRNA-143 acts as a tumor suppressor through Musashi-2/DLL1/Notch1 and Musashi-2/Snail1/MMPs axes in acute myeloid leukemia. J Transl Med 21: 309, 2023.
37. Osaki M, Takeshita F, Sugimoto Y, Kosaka N, Yamamoto Y, Yoshioka Y, Kobayashi E, Yamada T, Kawai A, Inoue T, *et al*: MicroRNA-143 regulates human osteosarcoma metastasis by regulating matrix metalloprotease-13 expression. Mol Ther 19: 1123-1130, 2011.
38. Zhang P, Zhang J, Quan H, Wang J and Liang Y: MicroRNA-143 expression inhibits the growth and the invasion of osteosarcoma. J Orthop Surg Res 17: 236, 2022.
39. Noguchi S, Mori T, Hoshino Y, Maruo K, Yamada N, Kitade Y, Naoe T and Akao Y: MicroRNA-143 functions as a tumor suppressor in human bladder cancer T24 cells. Cancer Lett 307: 211-220, 2011.
40. Kalaimani L, Devarajan B, Namperumalsamy VP, Veerappan M, Daniels JT and Chidambaranathan GP: Hsa-miR-143-3p inhibits Wnt-beta-catenin and MAPK signaling in human corneal epithelial stem cells. Sci Rep 12: 11432, 2022.
41. Yeh CH, Tseng R, Hannah A, Estrov Z, Estey E, Kantarjian H and Albitar M: Clinical correlation of circulating heat shock protein 70 in acute leukemia. Leuk Res 34: 605-609, 2010.
42. Valkenburg KC, Graveel CR, Zylstra-Diegel CR, Zhong Z and Williams BO: Wnt/β-catenin signaling in normal and cancer stem cells. Cancers (Basel) 3: 2050-2079, 2011.
43. Daskalakis M, Nguyen TT, Nguyen C, Guldberg P, Köhler G, Wijermans P, Jones PA and Lübbert M: Demethylation of a hypermethylated P15/INK4B gene in patients with myelodysplastic syndrome by 5-Aza-2'-deoxycytidine (decitabine) treatment. Blood 100: 2957-2964, 2002.
44. Tamm I, Wagner M and Schmelz K: Decitabine activates specific caspases downstream of p73 in myeloid leukemia. Ann Hematol 84 (Suppl): 47-53, 2005.